Numerical simulation of gas flow and heat transfer in a rough microchannel using the lattice Boltzmann method

Elaheh Dorari,* Majid Saffar-Avval,† and Zohreh Mansoori‡
Mechanical Engineering Department, Amirkabir University of Technology, Tehran, Iran
(Received 3 August 2015; revised manuscript received 13 October 2015; published 31 December 2015)

In microfluidics, two important factors responsible for the differences between the characteristics of the flow and heat transfer in microchannels and conventional channels are rarefaction and surface roughness which are studied in the present work. An incompressible gas flow in a microchannel is simulated two dimensionally using the lattice Boltzmann method. The flow is in the slip regime and surface roughness is modeled by both regular and Gaussian random distribution of rectangular modules. The effects of relative surface roughness height and Knudsen number on gaseous flow and heat transfer are studied. It was shown that as the relative roughness height increases, the Poiseuille number increases and the Nusselt number has a decreasing or increasing trend, depending on the degree of rarefaction. A comparison between the flow and heat transfer characteristics in regular and random distribution of surface roughness demonstrates that in regular roughness, circular flows are more pronounced; Poiseuille number is higher and Nusselt number is lower than that of its equivalent random roughness.

DOI: 10.1103/PhysRevE.92.063034 PACS number(s): 44.15.+a, 05.20.−y, 47.11.Qr, 51.10.+y

I. INTRODUCTION

In parallel with the development of micromachining technology, various experiments have been established in order to investigate transport phenomena in microchannels. Morini [1] has reviewed experimental results of single phase convective heat transfer in microchannels; he has shown that in addition to disagreement between the results of microscale experiments with conventional theories, microscale results are inconsistent themselves.

These inconsistencies are attributed to scale effects such as rarefaction, compressibility, electro-osmotic, viscous dissipation, property variation, surface roughness, and experimental uncertainties.

It is difficult and cost consuming to study these effects experimentally; a suitable theoretical approach contributes to study them distinctively through an inexpensive manner. Among these effects rarefaction and surface roughness are of significant importance for gaseous flow and heat transfer in microchannels.

The effects of surface roughness on rarefied gas flow and occasionally heat transfer in microgeometries are studied by different mathematical methods. Usami *et al.* [2], Sun and Faghri [3], and Lilly *et al.* [4] studied the effect of surface roughness on gaseous flow in a microchannel using the Direct simulation Monte Carlo (DSMC) method. Blanchard and Ligrani [5] determined the accommodation coefficient from rarefaction and roughness in rotating microscale disk flows by analytical solution of Naviers-Stokes equations. Li *et al.* [6] also used analytical solution of Navier-Stokes equations to study the effect of roughness on rarefied gas flow in long microtubes by modeling surface roughness as a porous film. Duan and Muzychka [7] studied the effect of corrugated surface roughness on developed laminar flow in microtubes using a perturbation method for analytical solution of Navier-Stokes equations. Zhang and Meng [8] established and solved analytically a modified Reynolds equation for taking account of surface roughness and rarefaction for various slider-bearing configurations. Ji *et al.* [9] and Khadem *et al.* [10] used the finite volume method to simulate gaseous flow and heat transfer in a rough microchannel. Turgay and Yazicioglu [11] simulated surface roughness by the finite element method and studied convective heat transfer in a microchannel. Yan *et al.* [12] combined the finite volume and finite element methods for three-dimensional simulation of gaseous flow in a micropipe. Using the molecular dynamics method, Davis *et al.* [13] and Cao *et al.* [14] investigated gas flow in rough microchannels.

The aforementioned methods have several disadvantages; DSMC usually suffers from expensive computational cost, high statistical noise, and multiple error sources in simulating low speed flows. Likewise, expensive computational cost of the molecular dynamics method limits its application in practice. Moreover, isothermal Navier-Stokes equations can be derived from the Boltzmann equation, using first-order approximation of the Chapman-Enskog expansion, and direct solution of these equations is appropriate for macroscopic flows.

During recent years, the lattice Boltzmann (LB) method has become popular as a mesoscopic numerical approach for microfluidics phenomena, especially for gaseous flow in microscale, due to its capability in simulating gas-particles interactions among themselves and with other phases such as solid walls. In addition, ease of complex geometry simulation is another advantage of this method. However, although thermal LB models have been developed well, to the authors' knowledge, the only study for rarefaction associated with surface roughness effect in microchannel is performed by Zhang *et al.* [15] in which temperature jump at rough gas-solid interface in Couette flow has been investigated using a double-distribution function thermal LB method. Other Lattice Boltzmann method (LBM) studies are limited to flow characteristics [16–19]. Chai *et al.* [16] studied rarefaction and surface roughness effect on gaseous flow. Surface roughness is modeled by rectangular elements and the results indicate that in a constant pressure difference at the inlet and outlet, increase in relative roughness height and roughness density leads to

*elahedoari@aut.ac.ir
†mavval@aut.ac.ir
‡z.mansoori@aut.ac.ir

Poiseuille number increase and mass flow rate decrease. Zhang *et al.* [17] used fractal Weierstrass-Mandelbrot function for surface roughness characterization and obtained results similar to [16], using a combination of bounce-back and specular slip boundary condition. However, as Suga [20] mentioned, the lattice Boltzmann boundary conditions have not been as sufficiently developed for complex geometries in high Knudsen number flows even though it is well developed for continuum assumption. So, using the typical slip boundary condition of bounce-back-specular reflection does not appropriately model the Weierstrass-Mandelbrot function. In both of the two above-mentioned studies, Known-pressure boundary conditions are used at the inlet and outlet which do not seem the best option for a surface roughness problem.

In this research the lattice Boltzmann approach has been used to study rarefaction and surface roughness effect on gaseous flow and heat transfer in a microchannel. Both regular and random roughness effects have been studied and compared.

II. MODEL DEVELOPMENT

A. Problem statement

Incompressible gaseous flow in the slip regime is considered between two parallel plates so that the Knudsen number range is $0.001 < \mathrm{Kn} < 0.1$, and the maximum Mach number is less than 0.01. Surface roughness is modeled as rectangular elements which are symmetrically distributed on the top and bottom walls in the fully developed region. Since the problem is symmetric, half of the channel is modeled as a numerical domain. A schematic of the two-dimensional (2D) flow through a channel with regular surface roughness with length $L$and height H is shown in Fig. 1.

Velocity distribution is uniform at the inlet and the Reynolds number is defined as $\mathrm{Re} = \frac{u_{\mathrm{in}} D_H}{\upsilon}$, where u_{in}, D_H, and υ are the inlet velocity, characteristic length, and kinematic viscosity, respectively. In microchannels, the Reynolds number at the inlet is usually small. Here, the inlet velocity of the gas flow is so chosen that the Reynolds number is equal to 0.1. The distance between the two plates is H, so the characteristic length is $D_h = 2H$. The ratio of microchannel length L to its height H is assumed to be 10, so that the fully developed conditions for both velocity and temperature are obtained. The inlet temperature of the gas flow is T_{in}. The constant temperature T_w is maintained on the upper and lower solid walls which is different from T_{in}. Air is assumed to be as the working fluid, so the Prandtl number is $\mathrm{Pr} = 0.71$.

At first the surface roughness is modeled by uniform rectangular elements that are regularly distributed along the channel surface, and then roughness elements are continuously distributed such that their height h and width w are chosen based on Gaussian distribution. Relative roughness height is defined as $e = \frac{h}{D_h}$ for regular roughness which is estimated to be in the range of [0.001–0.06] in microfluidic systems [9]; relative roughness height effect is also studied up to 0.06. For the regular rough elements, the distance between the center of two successive elements is called s which is equal to $s = 0.15H$ and the width w is assumed to be $0.06s$, in this study.

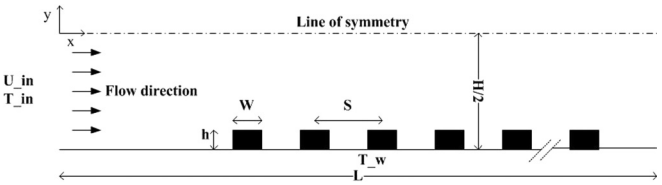

FIG. 1. Schematic of gas flow in a 2D microchannel with regular rough surface.

B. Mathematical formulation

The lattice Boltzmann method with its outstanding capability to capture the interfacial velocity slip and temperature jump by the use of different types of boundary conditions has been broadly applied to simulate gas slip flow in microchannels [21–23]. Therefore, it has been employed with a double-distribution function thermal model [24] in this study. The evolution equation of the lattice Boltzmann method for the velocity field can be written as follows [24]:

$$f_\alpha(\mathbf{x}_i + \mathbf{e}_\alpha \delta t, t + \delta t) = f_\alpha(\mathbf{x}_i, t) - \frac{1}{\tau_f}[f_\alpha(\mathbf{x}_i, t) - f_\alpha^{\mathrm{eq}}(\mathbf{x}_i, t)], \quad (1)$$

where f_α is the density distribution function at location $\mathbf{x}_i$ and direction α. In the above equation, f_α^{eq} is the local equilibrium distribution function that has an appropriately prescribed functional dependence on the local hydrodynamic properties and τ_f is the dimensionless relaxation time of the density distribution function. For the D2Q9 model the second order truncation of the equilibrium for the incompressible flow takes the form [24]

$$f_\alpha^{(\mathrm{eq})} = \rho \omega_\alpha \left[1 + \frac{(\mathbf{e}_\alpha \cdot \mathbf{u})}{c_s^2} + \frac{1}{2}\frac{(\mathbf{e}_\alpha \cdot \mathbf{u})^2}{c_s^4} - \frac{1}{2}\frac{(\mathbf{u} \cdot \mathbf{u})}{c_s^2}\right], \quad (2)$$

where ρ and $\mathbf{u}$ are the gas density and velocity, and c_s is the lattice sound speed which is equal to $1/\sqrt{3}$ when the uniform grid $\delta x = \delta y = \delta t = 1$ is used in the computational domain. Lattice directions α and their weighting factors ω_α should get sufficiently isotropic behavior; In order to achieve this requirement for D_2Q_9 model the weighting factors ω_α and discrete velocities $\mathbf{e}_\alpha$ are given as [24]

$$\begin{aligned} \mathbf{e}_{\alpha=0} &= 0, \\ \mathbf{e}_{\alpha=1-4} &= c\left(\cos\left[\frac{(\alpha-1)\pi}{2}\right], \sin\left[\frac{(\alpha-1)\pi}{2}\right]\right), \\ \mathbf{e}_{\alpha=5-8} &= c\sqrt{2}\left(\cos\left[\frac{(\alpha-5)\pi}{2} + \frac{\pi}{4}\right], \sin\left[\frac{(\alpha-5)\pi}{2} + \frac{\pi}{4}\right]\right), \end{aligned} \quad (3)$$

$$\omega_\alpha = \begin{cases} \omega_{\alpha=0} = \frac{4}{9} \\ \omega_{\alpha=1-4} = \frac{1}{9} \\ \omega_{\alpha=5-8} = \frac{1}{36} \end{cases}, \quad (4)$$

where $c = \frac{\delta x}{\delta t}$.

Since in the present study, kinematic viscosity and thermal diffusivity are considered constant, the decoupling double-distribution function (DDF) thermal model which is not capable of introducing high temperature variation into the momentum equation is suitable. In addition viscous dissipation and compression work are negligible due to small Mach number. In the DDF thermal model [24], when compression work and viscous dissipation terms are ignored, the lattice Boltzmann equation of the temperature field can be given by

$$g_\alpha(\mathbf{x}_i + \mathbf{e}_\alpha \delta t, t + \delta t) = g_\alpha(\mathbf{x}_i, t) - \frac{1}{\tau_g}[g_\alpha(\mathbf{x}_i, t) - g_\alpha^{\mathrm{eq}}(\mathbf{x}_i, t)], \tag{5}$$

where g_α is the temperature distribution function, τ_g is the dimensionless temperature relaxation time, and local equilibrium distribution function g_α^{eq} is

$$g_\alpha^{(\mathrm{eq})}(\mathbf{x}_i, t) = T(\mathbf{x}_i, t) f_\alpha^{\mathrm{eq}}(\mathbf{x}_i, t), \tag{6}$$

where $T(\mathbf{x}_i, t)$ is the temperature at position $\mathbf{x}_i$ and time t.

The macroscopic variables of the gas density ρ, velocity $\mathbf{u}$, and temperature T are defined as

$$\rho(\mathbf{x}_i, t) = \sum_{\alpha=0}^{8} f_\alpha(\mathbf{x}_i, t),$$
$$\mathbf{u}(\mathbf{x}_i, t) = \frac{1}{\rho(\mathbf{x}_i, t)} \sum_{\alpha=0}^{8} \mathbf{e}_\alpha f_\alpha(\mathbf{x}_i, t), \tag{7}$$
$$T(\mathbf{x}_i, t) = \frac{1}{\rho(\mathbf{x}_i, t)} \sum_{\alpha=0}^{8} \mathrm{g}_\alpha(\mathbf{x}_i, t).$$

In this model, the corresponding kinematic viscosity is $\upsilon = (\tau_f - 0.5)c_s^2 \delta t$ and the thermal diffusivity α_f is defined as $\alpha_f = (\tau_g - 0.5)c_s^2 \delta t$.

In microscale gas flow simulation by the lattice Boltzmann method, Guo *et al.* [25] have proposed the equation $\tau_f = \sqrt{\frac{6}{\pi}\frac{\mathrm{Kn}}{\Delta}} + \frac{1}{2}$ as a consistent relationship, where $\Delta = \frac{\delta x}{H}$. Accordingly, the relaxation time τ_g is given by $\tau_g = \frac{\tau_f - 0.5}{\mathrm{Pr}} + 0.5$, where the Prandtl number is $\mathrm{Pr} = \frac{\upsilon}{\alpha}$ [24].

Average friction factor fRe and Nusselt numbers Nu are calculated by average integration of local fRe and Nu along the microchannel walls.

$$f\mathrm{Re} = \frac{(P_i - P_{\mathrm{out}})D_H^2}{0.5\Delta x_i \mu \bar{u}_i}, \tag{8}$$

$$\mathrm{Nu} = \frac{D_H \left(\frac{\partial T}{\partial y}\right)_w}{T_w - T_{\mathrm{bulk}}}, \tag{9}$$

where $p = \rho c_s^2$, u_b, and T_b are the bulk velocity and temperature and u is the velocity component in the direction x.

C. Boundary condition

For the inlet and outlet hydrodynamic boundary conditions, a nonequilibrium bounce-back model [26], normal to the boundary, is applied. For the temperature boundary conditions, constant temperature boundary condition at the inlet and second order extrapolation at the outlet is applied as proposed in [24]. Regarding the wall boundary condition, in the slip flow regime, there are fewer interactions between the gas molecules and the walls than those in the core of the gas flow due to rarefaction, so thermodynamic disequilibria appear in the near wall region and a velocity slip and a temperature jump must be considered at the solid walls. In this study the combination of bounce-back and specular reflection [27] in expression (10), and the combination of bounce-back and diffuse reflection [28] in expression (11) has been chosen to simulate velocity slip and temperature jump, respectively.

$$\begin{aligned} f_2 &= f_4, \\ f_5 &= r_f f_7 + (1 - r_f) f_8, \\ f_6 &= r_f f_8 + (1 - r_f) f_7. \end{aligned} \tag{10}$$

$$\begin{aligned} g_2 &= \sigma_g g_{4\ \theta_w, u_w}^{\mathrm{eq}} + (1 - \sigma_g) g_4, \\ g_5 &= \sigma_g g_{5\ \theta_w, u_w}^{\mathrm{eq}} + (1 - \sigma_g) g_8, \\ g_6 &= \sigma_g g_{6\ \theta_w, u_w}^{\mathrm{eq}} + (1 - \sigma_g) g_7, \end{aligned} \tag{11}$$

where r_f is the fraction of molecules that have bounce-back reflection and $1 - r_f$ indicates the fraction of molecules with specular reflection at the wall. Thermal accommodation coefficient σ_g is the fraction of molecules that reach the equilibrium temperature of the wall during collision with the wall, and the fraction $(1 - \sigma_g)$ of the molecules sustain their own temperature before collision.

D. Case validation

In the simulation, a grid independence test using several different mesh sizes is conducted and an appropriate mesh size for the next studies is selected so that grid independency is assured. To validate the LBM results with combination of bounce-back specular reflection slip boundary condition adopted in the present study, the Poiseuille gas flow in a smooth microchannel is simulated. In this case, locally fully developed flow is simulated, and slip coefficient r_f is chosen as the proposed expression (12) in Ref. [21], so that the obtained results correspond with the second order analytical solution of friction factor (13) in a smooth microchannel.

$$r_f = \left\{1 + \sqrt{\frac{\pi}{6}}\left[\frac{\Delta^2}{4Kn} + A_1 + \left(2A_2 - \frac{8}{\pi}\right)\mathrm{Kn}\right]\right\}^{-1}, \tag{12}$$

$$f\mathrm{Re} = \frac{96}{1 + 6A_1\mathrm{Kn} + 12A_2\mathrm{Kn}^2}, \tag{13}$$

where $A_1 = 2\zeta/\sqrt{\pi}$ and $A_2 = (1 + 2\zeta^2)/\pi$, with $\zeta = 1.016$ for the fully diffusive case [21].

Figure 2 compares the Poiseuille number Po of gas flow in a smooth microchannel between the numerical results and analytical solution. As seen from the figure, the numerical results obtained by LBM in the present work are in good agreement with the analytical solution.

In another validation, a flow at $\mathrm{Re} = 0.01$ which is confined between two parallel plates, with flow and thermal boundary conditions similar to the ones in Ref. [29], is considered. The Prandtl number is fixed as $\mathrm{Pr} = 0.7$. Table I compares the value of fully developed Poiseuille and Nusselt number for different Kn values with those in Refs. [29,30], which show good agreement between the results.

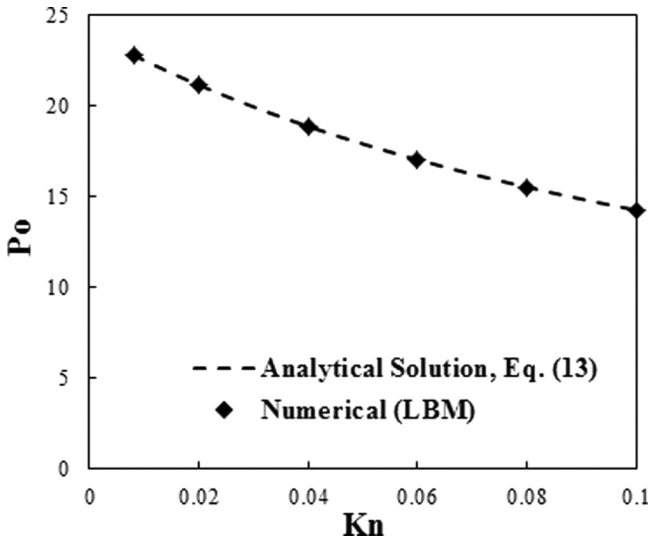

FIG. 2. Comparison of Poiseuille number by LBM with analytical solution.

III. RESULTS AND DISCUSSION

In this section, the effects of wall roughness and rarefaction on flow and heat transfer are investigated and discussed. As anyone knows, the thermohydrodynamic results are strongly dependent on both slip coefficient and thermal accommodation coefficient. In order to avoid the effect of these constants on obtained results, these two parameters are considered constant and equal to 0.6 and 1, respectively.

A. Effect of relative surface roughness height

Figure 3 illustrates the streamline patterns inside the rough microchannel. It is shown that streamlines are distorted in the presence of surface roughness; this deviation is more pronounced in the vicinity of the roughness elements and is caused as a result of expansion and compression of the flow. In addition, recirculating flows are generated between the roughness elements due to the pressure vibration, and this recirculation zone becomes larger up to the point where the roughness height increases.

Figure 4 plots the average Poiseuille number in the fully developed region of gas flow as a function of roughness height e. It is noticed that the roughness height plays a significant role in boundary interaction and frictional drag. Recirculation zones can be regarded as dead zones with velocity slips near zero, causing frictional drag increase. Besides, as the relative roughness height increases, dead zones develop, slip velocity at the valleys decreases, and pressure vibration increases and all these contribute to increase in Poiseuille number as shown in Fig. 4. However, the surface roughness has more significant effect on a lower Kn flow. In other words, an increase in fRe under a lower Kn number is more significant than that under a higher Kn number, since in lower Kn number flows, the collision between rough walls and gas molecules occur more often than those for higher Kn number gas flow. For the gas with a lower Kn number, the stagnation region between roughness elements causes a greater pressure drop and a higher increase in fRe.

Surface roughness and rarefaction exert a remarkable effect on gas flow field and subsequently results in changes in heat transfer characteristics that are a function of flowfield. Regarding the effect of surface roughness, in valleys, the

TABLE I. Comparison of fully developed Nu and Po at different Kn numbers.

Kn	Po[a]	Po[b]	Po[c]	Nu[a]	Nu[b]	Nu[c]
0.015	21.83	21.69	21.69	7.42	7.48	7.48
0.03	20.61	19.81	19.81	7.03	7.07	7.07
0.046	18.2	18.11	18.11	6.60	6.63	6.63

[a]Reference [30].
[b]Reference [29].
[c]Present study.

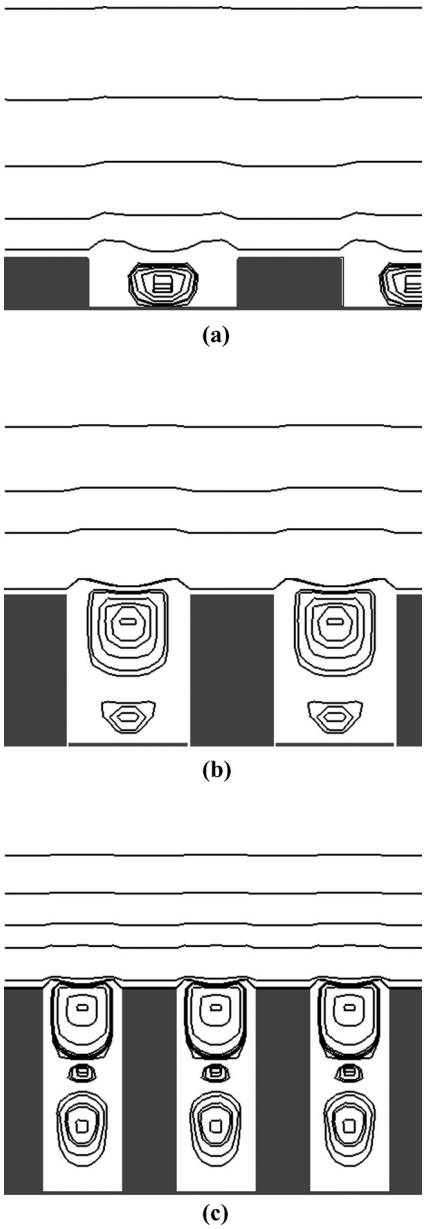

FIG. 3. Streamline contours for Kn = 0.03, (a) $e = 1\%$, (b) $e = 3\%$, (c) $e = 6\%$.

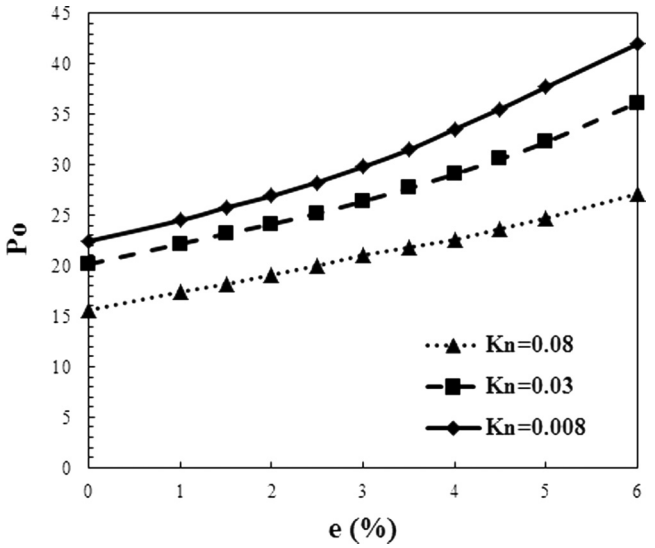

FIG. 4. Effect of relative roughness height on average fRe for rarefied gas flow.

temperature gradient is very low due to recirculating flows which act like heat transfer insulation. In addition, the average velocity in compressed cross sections of the microchannel on the top of the roughness elements increases according to the law of the mass conservation along the channel, which further leads to increase in local slip velocity on top of the roughness elements. Increase in slip velocity in these cross sections yields to local heat transfer enhancement. As the relative roughness height increases, this local heat transfer enhancement becomes more pronounced; on the other hand recirculating flows in valleys become more stagnant and provide more insulation. It is also observed that roughness height increase does not contribute to heat transfer surface increase. This is because as the roughness height increases the entire space of the valleys is

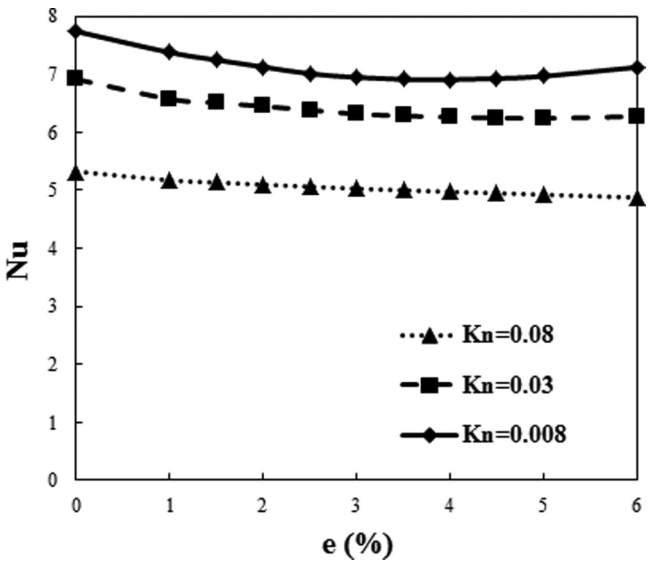

FIG. 5. Effect of relative roughness height on average Nu for rarefied gas flow.

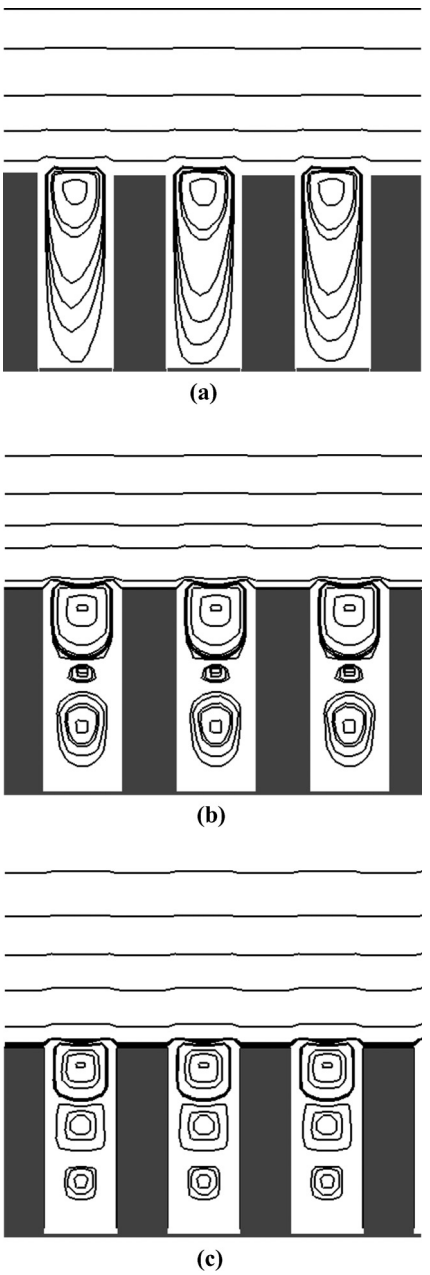

FIG. 6. Streamline contours for $e = 6\%$, (a) Kn $= 0.008$, (b) Kn $= 0.03$, (c) Kn $= 0.08$.

filled with stagnant flow with insulation effect, so the effective heat transfer area remains constant, as shown in Fig. 3.

Figure 5 plots the effect of relative roughness height on average Nu for rarefied gas flow. When Kn $= 0.008$, Nusselt number decreases as the relative roughness height increases up to $e = 4\%$, which indicates that the thermal insulation effect is more significant than the velocity increase effect. Further roughness height increase up to $e = 6\%$ brings about more heat transfer enhancement due to velocity increase which reverses the Nusselt number, changing the trend from decreasing to increasing. A similar trend occurs for Nusselt number change in Kn $= 0.03$, with a minimum relative roughness height $e = 5\%$. As the rarefaction effect increases, surface roughness effect becomes less important due to less interaction between

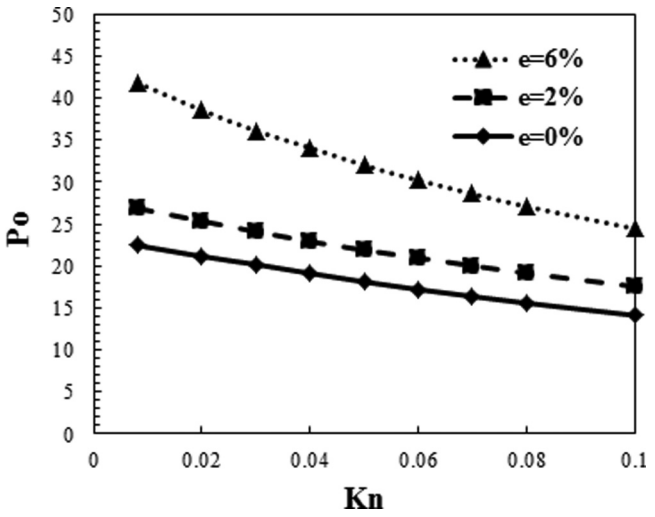

FIG. 7. Effect of rarefaction on average *f*Re for different surface roughness.

the gas molecules and walls, so the effect of slip velocity increase due to average velocity increase in compressed cross sections becomes less significant. Consequently, heat transfer decreasing effects dominate in gas flow with higher Kn numbers, as the roughness height increases, so that in Kn = 0.08 the Nu number changing trend is decreasing up to $e = 6\%$.

B. Effect of rarefaction

Streamline patterns in microchannel for different Kn numbers are shown in Fig. 6. It is seen that near continuum flow when Kn = 0.008, there is only one recirculating flow in the valleys. As the Kn number increases, separated recirculating flows occur and develop. This separation is due to the rarefaction. In fact, as the Knudsen number increases, mean free path length increases and small separated recirculating flows develop in the entire place of the valleys.

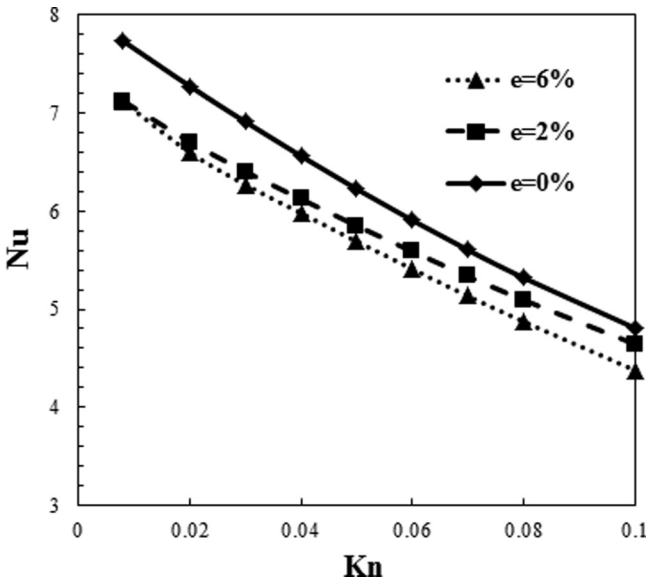

FIG. 8. Effect of rarefaction on average Nu for different relative surface roughness heights.

The effect of rarefaction on the Poiseuille number is shown in Fig. 7. It is noticed that as the Knudsen number increases, the Poiseuille number decreases in both smooth and rough microchannel. In fact, rarefaction enhancement leads to less interaction between gas molecules and walls, and less interaction leads to weaker frictional drag and less pressure drop in comparison to near continuum state Kn = 0.008.

Figure 8 plots the Nusselt number change versus Knudsen number increase. An increase in Kn number results in an increase in slip velocity and temperature jump which further brings about heat transfer increase and decrease, respectively. It is observed that as rarefaction effect increases, heat transfer rate decreases. This reduction in heat transfer rate indicates that the heat transfer reduction effects dominate heat transfer enhancement factors in both smooth and rough microchannels.

C. Effect of roughness distribution

Although regular surface roughness simulation contributes to the study of different phenomena, surface roughness has a random structure. In order to examine the effect of random

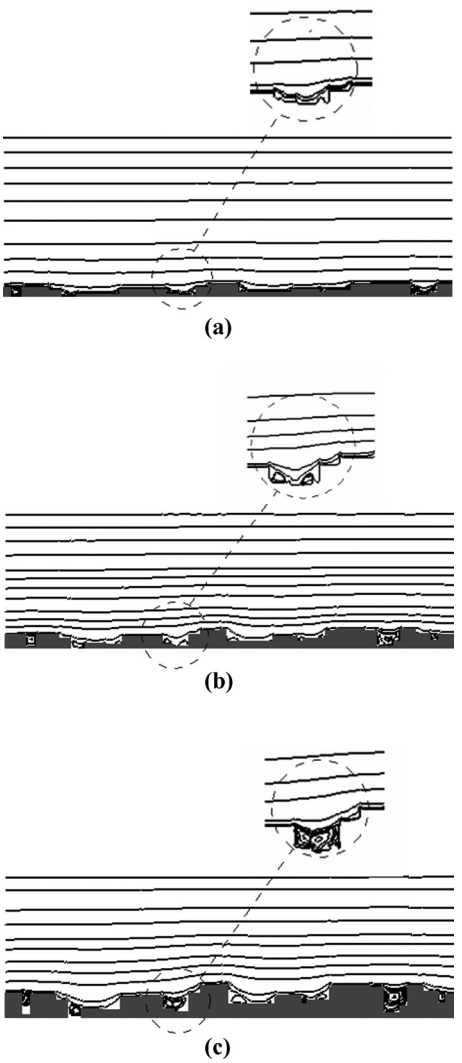

FIG. 9. Streamline contours for Kn = 0.03, (a) e = 1.12%, (b) e = 1.54%, (c) e = 3.17%.

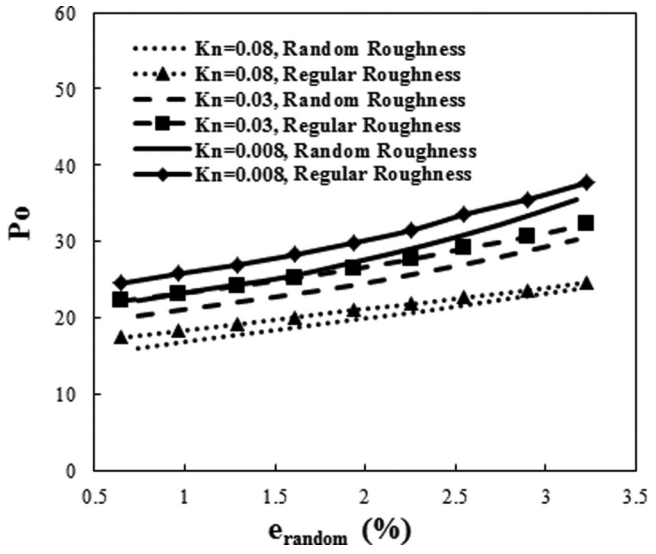

FIG. 10. Comparison between Poiseuille number for regular and random surface roughness.

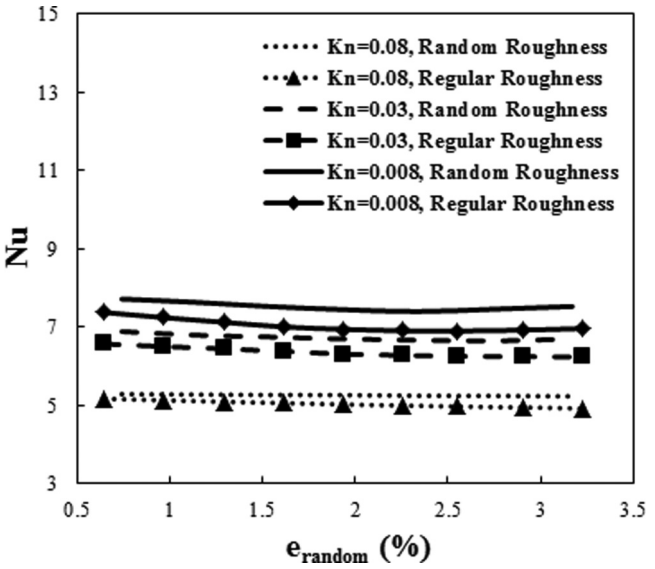

FIG. 11. Comparison between Nusselt number for regular and random surface roughness.

roughness distribution on fluid flow characteristics, in this section roughness heights and widths are obtained from Gaussian distribution, so that a Box-Muller [31] transformation function is used to generate a set of random variables with a Gaussian distribution with zero mean and a standard deviation of 1; after applying a translation, scaling, and a floor function on them, respectively, they are used as heights and widths of the roughness elements. Relative surface roughness height is defined as the area of the roughness elements per unit length of the channel $e_{\text{random}} = 100 \times A_{\text{Roughness}}/(H L_{\text{Roughness}})$.

Figure 9 illustrates flow streamlines in microchannel with random rough surface. It is noticed that in this kind of roughness distribution, recirculation zones are weaker and limited in comparison to regular roughness distribution; consequently, less frictional drag is imposed on gas flow, as plotted in Fig. 10. This might seem in contrast to the results obtained by Cao *et al.* [14], who reported that friction coefficient of flow in randomly triangular roughness channels is larger than that in regular rectangular ones. However, in their study no recirculating flow was observed. It is also observed that as rarefaction increases, the difference between the Poiseuille number obtained from regular roughness and random roughness decreases; this is because by increasing rarefaction, the surface profile is weakly captured by gas flow, and surface effects become less important.

Figure 11 compares average Nusselt number in a microchannel with regular and random wall roughness. It is noticed that the Nusselt number for a microchannel with random surface roughness is more than the Nusselt number for regular wall roughness. As shown in Fig. 9, in random roughness distribution less recirculating flows occur which means there is less thermal insulation area, so the heat transfer improves. It is also noticed that the Nusselt number for a smooth surface is more than the Nusselt number for each type of roughness distribution studied here.

IV. CONCLUSION

The effects of rarefaction and wall roughness on flow and heat transfer inside a two-dimensional microchannel is studied using the lattice Boltzmann method. It was observed that in the presence of surface roughness, recirculation zones resist flow and relative roughness height increase leads to increased Poiseuille number. The relative roughness height effect is more pronounced in lower Knudsen number flows. Recirculation zones provide heat transfer insulation and lead to Nusselt number decrease up to where relative roughness height is $e = 4\%$, $e = 5\%$, and $e = 6\%$ for $\text{Kn} = 0.008$, $\text{Kn} = 0.03$, and $\text{Kn} = 0.08$, respectively. For the case of random roughness distribution, the Poiseuille number is less than its equivalent regular roughness and the Nusselt number is more than that. This is because fewer recirculation zones occur in random roughness, so causing weaker flow resistance and thermal insulation effect.

[1] G. L. Morini, Int. J. Therm. Sci. **43**, 631 (2004).
[2] M. Usami, T. Fujimoto, and S. Kato, Trans. Jpn. Soc. Mech. Eng., Ser. B **54**, 1042 (1988).
[3] H. Sun and M. Faghri, Numer. Heat Transfer, Part A **43**, 1 (2003).
[4] T. C. Lilly, J. A. Duncan, S. L. Nothnagel, S. F. Gimelshein, N. E. Gimelshein, A. D. Ketsdever, and I. J. Wysong, Phys. Fluids **19**, 106101 (2007).
[5] D. Blanchard and P. Ligrani, Phys. Fluids **19**, 063602 (2007).
[6] W.-L. Li, J.-W. Lin, S.-C. Lee, and M.-D. Chen, J. Micromech. Microeng. **12**, 149 (2002).
[7] Z. Duan and Y. Muzychka, Fluids Eng. **130**, 031102 (2008).
[8] W.-M. Zhang and G. Meng, IEEE/ASME Trans. Mechatronics **14**, 465 (2009).

[9] Y. Ji, K. Yuan, and J. Chung, Int. J. Heat Mass Transfer **49**, 1329 (2006).
[10] M. Khadem, M. Shams, and S. Hossainpour, Int. Commun. Heat Mass Transfer **36**, 69 (2009).
[11] M. Turgay and A. G. Yazicioglu, Numer. Heat Transfer, Part A **56**, 497 (2009).
[12] H. Yan, W-M. Zhang, Z-K. Peng, and G. Meng, Microfluid. Nanofluid. 1 (2014).
[13] D. H. Davis, L. L. Levenson, and N. Milleron, J. Appl. Phys. **35**, 529 (1964).
[14] B.-Y. Cao, M. Chen, and Z.-Y. Guo, Int. J. Eng. Sci **44**, 927 (2006).
[15] C. Zhang, Z. Deng, and Y. Chen, Int. J. Heat Mass Transfer **70**, 322 (2014).
[16] Z. Chai, Z. Guo, L. Zheng, and B. Shi, J. Appl. Phys. **104**, 014902 (2008).
[17] C. Zhang, Y. Chen, Z. Deng, and M. Shi, Phys. Rev. E **86**, 016319 (2012).
[18] L. Chao-Feng and N. Yu-Shan, Chin. Phys. B **17**, 4554 (2008).
[19] C. Kunert and J. Harting, Phys. Rev. Lett. **99**, 176001 (2007).
[20] K. Suga, Fluid Dyn. Res. **45**, 034501 (2013).
[21] Z. Guo, B. Shi, T. S. Zhao, and C. Zheng, Phys. Rev. E **76**, 056704 (2007).
[22] F. Verhaeghe, L.-S. Luo, and B. Blanpain, J. Comput. Phys. **228**, 147 (2009).
[23] G. Tang, W. Tao, and Y. He, Phys. Fluids **17**, 058101 (2005).
[24] A. A. Mohamad, *Lattice Boltzmann Method: Fundamentals and Engineering Applications with Computer Codes* (Springer Science & Business Media, London, 2011).
[25] Z. Guo, T. Zhao, and Y. Shi, J. Appl. Phys. **99**, 074903 (2006).
[26] Q. Zou and X. He, Phys. Fluids **9**, 1591 (1997).
[27] S. Succi, Phys. Rev. Lett. **89**, 064502 (2002).
[28] L. Zheng, Z. Guo, and B. Shi, Europhys. Lett. **82**, 44002 (2008).
[29] C. Shu, X. Niu, and Y. Chew, Stat. Phys. **121**, 239 (2005).
[30] H. P. Kavehpour, M. Faghri, and Y. Asako, Numer. Heat Transfer, Part A **32**, 677 (1997).
[31] G. E. Box and M. E. Muller, Ann. Math. Stat. **29**, 610 (1958).